Electrospun Organic Nanofiber Electronics and Photonics

Himchan Cho, Sung-Yong Min, Tae-Woo Lee*

Organic nanofibers (ONFs) have attracted much interest as one-dimensional functional units in various research fields with their unique advantages. Among many fabrication methods for them, electrospinning has been in the spotlight recently because of its simplicity and versatility. In this paper, first we introduce the principle, advantages, and conditions of electrospinning and then review recent studies about electronic and photonic applications of electrospun ONFs, including organic light-emitting diodes, organic photovoltaics, organic field-effect transistors, lasers, and waveguides. Finally, conclusion and our suggestions for further research are given.

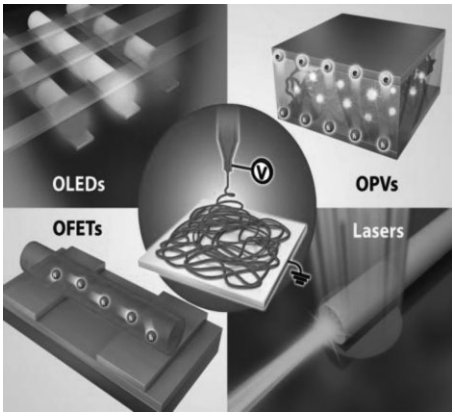

1. Introduction

During the last two decades, organic semiconductors (OSCs) have generated considerable research interests in the fields of electronics[1–3] and photonics[4–6] because OSCs have diverse advantages such as low-cost and lightweight products, large-area and high-throughput processes, easy control of molecular properties, and good compatibility with flexible substrates. Most of this research, however, has examined only three-dimensional (3D) bulk systems. Research into one-dimensional (1D) organic systems,[7] including organic nanofibers (ONFs), is at a comparatively early stage. Many researchers have been studying ONF systems to make the most of their novel characteristics (Figure 1a).

ONFs may be the most suitable subject for fundamental research on OSCs. For example, Nguyen et al. systematically demonstrated that interchain energy transfer occurs more quickly than intrachain energy migration in ONFs using single-chain polymer nanofiber arrays in the templates.[8] The increased stacking order of π-conjugated molecules in ONFs gives them charge transport mobility and conductivity that are superior to those of thin films, especially for single-crystalline ONFs.[7,9] Also, the large surface-to-volume ratio of ONFs guarantees improved efficiency and sensitivity in energy harvesting[10–12] and chemical sensing.[13,14] Furthermore, light-emitting ONFs are expected to have important functions, such as 1D light sources in nanoscale photonic circuits. For further understanding of fundamental properties of ONFs, we encourage to read some other well-established review papers.[7,15,16]

1D micro- and nano-structures in forms of wires or fibers have been prepared using numerous methods, including electrospinning[17–19], template-assisted method,[20] self-assembly,[21] direct drawing,[22] nanoimprint lithography,[23] physical vapor transport,[24] scanning probe lithography,[25] and nanofluidics[26] (Figure 1b). In this paper, we primarily review recent progress in electronics and photonics based on ONFs drawn using electrospinning techniques. We review the principle, materials and advantages of electrospinning in Section 2. Then, we discuss the application of electrospun ONFs to organic

H. Cho, S.-Y. Min, Prof. T.-W. Lee
Department of Materials Science and Engineering, Pohang University of Science and Technology (POSTECH), San 31, Hyoja-dong, Nam-gu, Pohang, Gyeongbuk 790-784, Korea
E-mail: twlee@postech.ac.kr

DOI: 10.1002/mame.201200364

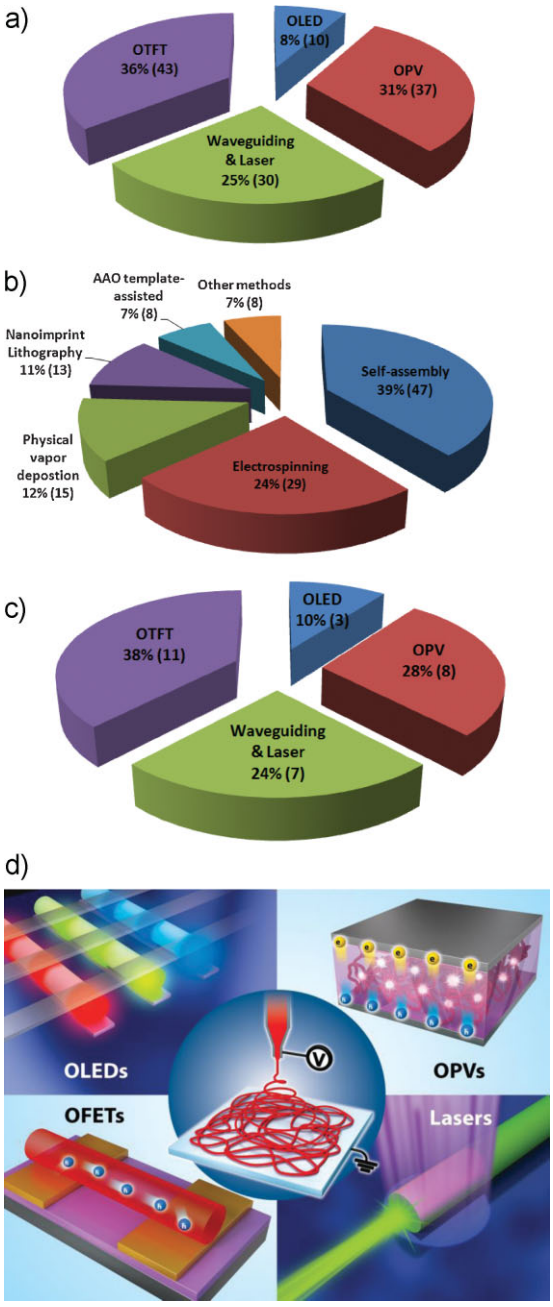

Figure 1. Statistics of literature published on (a) electronic and photonic applications of ONFs, (b) methods of fabricating ONFs in electronic and photonic applications, (c) electronic and photonic applications of ONFs fabricated by electrospinning. The literature used in the statistics was searched mainly using a premier research database platform, Thomson Reuters Web of Knowledge℠ (http://www.isiknowledge.com) (representative search keywords: ONFs, polymer nanofibers, nanowires, light-emitting, photovoltaics, field effect transistors, lasers) (d) various applications of electrospun ONFs to electronic and photonic devices.

Himchan Cho received his B.S. in Materials Science and Engineering from Pohang University of Science and Technology (POSTECH) in 2012. He is a graduate student in POSTECH since 2012. His current research work is focused on optoelectronic and photonic applications of controllable organic nanofibers.

Sung-Yong Min received his B.S. in Materials Science and Engineering from Pohang University of Science and Technology (POSTECH) in 2010. He is a graduate student in POSTECH since 2010. His current research work is focused on controllable organic nanofibers for nanolithography and electronic applications in large-area.

Tae-Woo Lee is an associate professor in the department of the materials science and engineering at Pohang University of Science and Technology (POSTECH), Korea. He received his Ph.D in chemical engineering from KAIST, Korea in February 2002. Then, he joined Bell Laboratories, USA as a postdoctoral researcher in 2002. From September 2003 to August 2008, he worked in Samsung Advanced Institute of Technology, Samsung Electronics as a member of research staff. He received a prestigious Korea Young Scientist Award from the President of Korea in 2008. He is author and co-author of 100 papers including Nature Photonics, PNAS, Angewandte Chemie, Advanced Materials, Nano Letters, and Advanced Functional Materials, as well as inventor and co-inventor of 214 patents (94 Korean patents and 124 international patents). His research focuses on printed and organic electronics based on organic and carbon materials for flexible electronics, displays, solid-state lightings, and solar energy conversion devices. Recently, he has performed research on organic nanofiber electronics such as transistors, light-emitting diodes, and photovoltaic cells.

light-emitting diodes (OLEDs), organic photovoltaics (OPVs), organic field-effect transistors (OFETs), lasers, and waveguides in terms of the material, electrical, and optical characteristics with reference to several representative advanced research reports (Section 3–6). We provide a conclusion and propose future work on electrospun ONFs in Section 7.

2. Electrospinning

Electrospinning is a useful technique to fabricate continuous ultrathin nanofibers from organic or organic/inorganic composite solutions.[17–19] It is an easy, simple

and inexpensive process which does not require any template, expensive equipment, or additional processing. This method has great versatility and potential in that any functional additive can be mixed in ONFs, and that high-throughput industrial processes can be possible. With these advantages, it has been widely investigated for use in electronics,[27] photonics,[28] bio-engineering,[29] energy applications,[10–12] filters,[30] and sensors[13,14] (Figure 1c). However, a fine shape control and precise positioning of individual ONFs, which was previously achieved by sophisticated scanning probe lithography and nanofluidics, are challenges for applications of electrospinning.[25,26] Therefore, if it is possible to develop the novel process that enables an individual position control of semiconducting ONFs, electrospinning can be an excellent choice for fabricating ONF devices.

The basic electrospinning setup consists of a spinneret, a grounded collector and a high-voltage power supply (Figure 2a). Briefly, the process is as follows. A syringe containing prepared solution is mounted with the spinneret. A syringe pump continuously feeds the solution at a constant rate while a sufficiently high voltage is applied to the spinneret. Then, the droplet that hangs from the nozzle tip becomes evenly charged, so electrostatic repulsion and external electric forces shape the droplet into a Taylor cone. When electric force overcomes the surface tension of the solution, the jet forms at the tip of Taylor cone, elongates with a whipping motion and tapers into nanofibers as the solvent evaporates. Finally, a nonwoven mat of randomly oriented continuous ONFs accumulates on the substrate. Many well-organized papers describe this process in detail.[17–19,31,32]

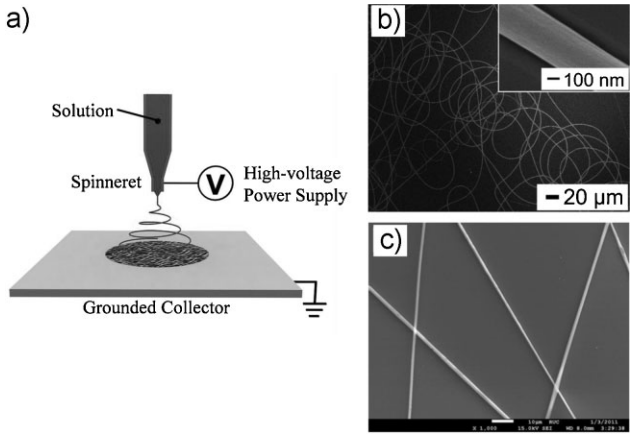

Figure 2. (a) Schematic diagram of a typical electrospinning setup. (b) Scanning electron microscope (SEM) image of electrospun blend fibers of P3HT and PCL using a single nozzle, P3HT/PCL (80:20 w/w); inset: higher-magnification SEM images of the fibers.[37] (c) SEM image of electrospun rubrene/PEO blend nanofibers having ≈600-nm diameter.[99] Reproduced with permission.[37,99] Copyright 2009 The Royal Society of Chemistry[37] and 2012, American Institute of Physics.[99]

Although the process is quite straightforward, various processing parameters must be carefully considered to achieve spinnable regime (normally, the word "spinnability" refers to the ability to form continuous uniform nanofibers) and control their diameters and morphologies. These parameters can be classified into solution parameters [including concentration, molecular weight (MW)] and dynamic parameters (including applied voltage, feeding rate, tip-to-collector distance, solvent volatility, electrical conductivity, humidity).[17–19,31,32] Although both of them significantly influences the spinnability, from a fundamental point of view, solution parameters are the more decisive factors. That is because the proper control of concentration and MW can basically prevent the breakage of extruded jet which limits continuous fiber formation. Strong entanglement between polymer chains effectively provides sufficient intermolecular force to the solution so that the jet can overcome a capillary breakup into droplets by surface tension, which is referred as "Rayleigh instability". Therefore, to overcome Rayleigh instability, the concentration of polymer solutions must be sufficiently high to connect the molecules into continuous chains with enough chain entanglement. However, the concentration should be in optimum range because too high concentration can cause fiber breakage due to fracture with overlong relaxation time[31] and nozzle clogging with the solidified polymer at the nozzle tip. In addition, high MW and narrow molecular weight distribution (MWD) can be a great help to increase molecular connectivity.[31,32] Polymers with high MW and narrow MWD provide uniform fiber formation at relatively lower concentration as compared to polymers with low MW and broad MWD.[32] High-MW polymers have large hydrodynamic radii, which make strong chain entanglement in the solution (Figure 3a–c). Narrow MWD can prevent the presence of weak chain link, which can cause fiber breakage during the stretching process (Figure 3d, e).[32]

Poly(3-hexylthiophene) (P3HT) is one of the most typical semiconducting polymers which has been actively studying in ONF electronics.[21,23,33–41] However, commonly used P3HTs cannot provide enough chain entanglement and cannot overcome Rayleigh instability due to their rigid molecular structure[33] and relatively low MWs ($19.4\,\text{kDa} \leq \overline{M}_w \leq 87\,\text{kDa}$).[36–41] P3HT with high-MW ($\overline{M}_w \geq 87\,\text{kDa}$) and narrow MWD, which may be more spinnable, is rarely used because of low solubility, difficulty of synthesis,[42] and poor electrical characteristics.[43–45] P3HT in the relatively lower MW range has shown greater field-effect mobility ($30\,\text{kDa} \leq \overline{M}_n \leq 40\,\text{kDa}$)[43] and photovoltaic efficiency ($18\,\text{kDa} \leq \overline{M}_n \leq 34\,\text{kDa}$ or $\overline{M}_w = 55\,\text{kDa}$)[44,45] than those in higher MW range.

Hence, it is hard to fabricate electrospun ONFs with pure P3HT solutions.[33] Other low-MW polymers and small molecules have the same problem. Therefore,

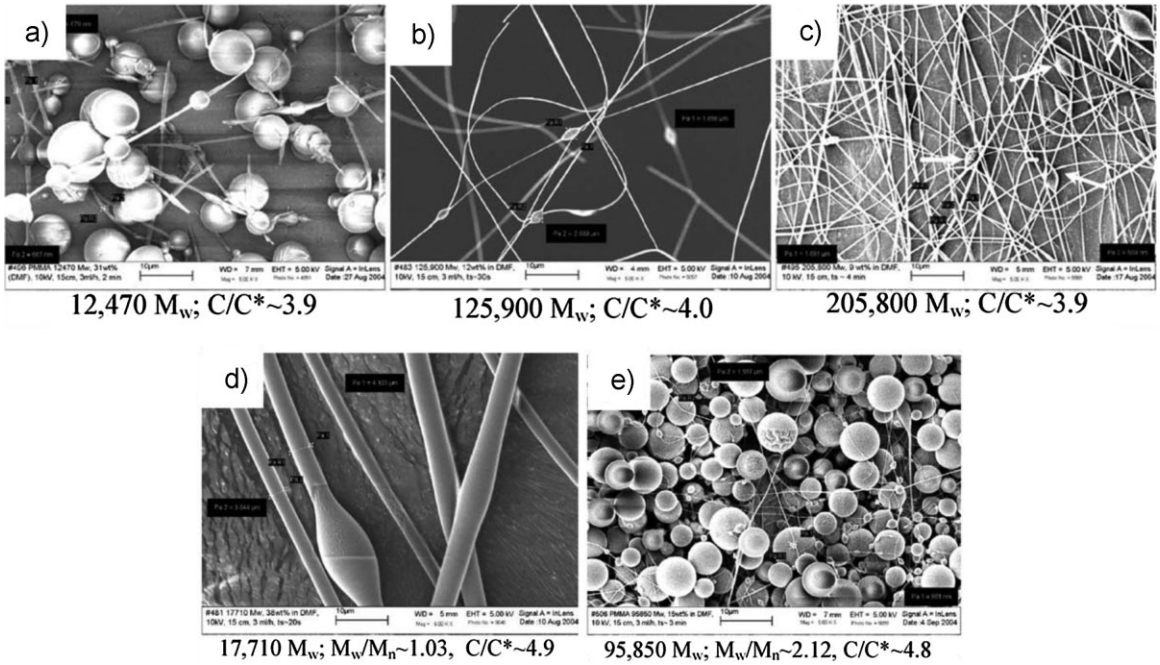

Figure 3. SEM images of electrospun PMMA nanofibers from solutions in the semi-dilute entangled regimes (a)–(c) at $c/c^* \approx 3.9$–4.0 for three different $\overline{M}_w$, 12 470, 125 900, and 205 800. (d,e) at $c/c^* \approx 4.8$–4.9 for polymers with the narrow ($\overline{M}_w/\overline{M}_n \approx 1.03$) and broad ($\overline{M}_w/\overline{M}_n \approx 2.12$) MWD. All the scale bars in the images correspond to 10 μm. Reproduced with permission.[32] Copyright 2005, Elsevier Ltd.

high-MW polymers, such as poly(vinyl pyrrolidone) (PVP),[33,41,46–48] polystyrene (PS),[49] poly(ε-caprolactone) (PCL),[37,38] poly(methyl methacrylate) (PMMA),[40] and poly(ethylene oxide) (PEO),[49,50] have been usually mixed with conjugated polymers as a matrix to induce more chain entanglements and establish sufficient jet-holding force for fiber formation (Figure 2b, c). Coaxial electrospinning, which employs two-capillary spinneret, can be a very useful method for fiber formation because a solution of matrix polymer can be supplied independently by the outer spinneret, regardless of the material inside.[33,37,40,41,51] For example, Li et al. demonstrated that poly(2-methoxy-5-(2-ethylhexoxy)-*p*-phenylenevinylene) (MEH-PPV)/P3HT blend nanofibers could be formed by coaxial electrospinning. They put PVP solution into the outer spinneret and fabricated core–shell ONFs which contained MEH-PPV/P3HT blend inside the core region.[41]

3. OLEDs Based on Electrospun ONFs

The OLED technology has been advancing enormously as a result of the development of OSCs.[52–57] OLEDs have several inherent advantages over conventional liquid crystal displays, including simpler fabrication process, lighter weight, thinner display panel, potentially lower manufacturing cost, wider viewing angle, faster response time, and potential flexibility; these advantages make OLEDs the most promising candidates for next-generation display. However, improving operational lifetime and reducing fabrication cost for large-area device array are the remaining challenges of OLED devices.

Current research on OLEDs has mainly focused on two-dimensional (2D) thin film devices.[52–57] Active study of OLEDs that use 1D light-emitting ONFs has been impeded by some drawbacks. First, charge injection into active layers can be hindered due to the circular geometry of ONFs.[7] Also, this fiber-type active layers can cause short circuit between two electrodes in conventional vertical OLED structure, because they cannot cover entire device area. Furthermore, the large surface-to-volume ratio of ONFs can act as an obstacle for 1D fiber-based OLED because of their sensitivity to oxygen and humidity. To overcome these obstacles, further research about the development of device structure and passivation method suitable for 1D light-emitting structure must be followed. Nevertheless, ONF-based OLEDs have great academic significance in that they can function as 1D subwavelength light sources in nano-size optoelectronic systems as well as in lab-on-chip devices.[7,16,58,59]

Moran-Mirabal et al. fabricated electrospun light-emitting nanofibers of ruthenium (II) tris(bipyridine) ($[Ru(bpy)_3]^{2+}(PF_6^-)_2$) and PEO mixture.[60] The nanofibers were laid on Au interdigitated electrodes (IDEs) with a gap of 5 μm or 500 nm, and emitted highly confined light of 240×325 nm^2 or smaller area between IDEs at turn-on

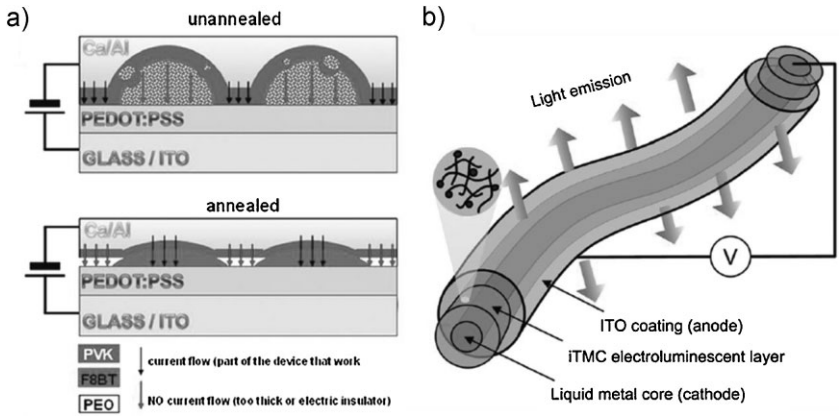

Figure 4. (a) Schematic diagrams of the device architectures of unannealed and annealed devices.[49] (b) Schematic structure of iTMC-based electro-luminescent nanofibers with liquid metal core, iTMC electroluminescent layer and ITO coating.[51] Reproduced with permission.[49,51] Copyright 2011, American Chemical Society.

voltages of 10 and 3.2 V, respectively. Similarly, Yang et al. recently used coaxial electrospinning to develop single core–shell fiber OLEDs based on an ionic transition-metal complex (iTMC) (Figure 4b).[51] A galinstan liquid metal core and a $([Ru(bpy)_3]^{2+}(PF_6^-)_2)$/PEO blend shell were co-electrospun to form the cathode and an electroluminescent layer, respectively. Afterwards, an indium tin oxide (ITO) anode layer was deposited by evaporation; the electroluminescence of the device was turned on at 4.2 V. Particularly interesting point of this work is that it has realized the direct fabrication of 1D electroluminescent device via electrospinning. However, neither of these papers reported the efficiency or brightness of the devices.[51,60]

Vohra et al. prepared electrospun F8BT/PEO blend nanofibers and used them as active layers in OLEDs (Figure 4a).[49] The authors successfully solved the charge injection problem in ONF layers using an annealing step, which flattens the active layers into ribbonlike morphology and separates PEO from the ONFs. The measured luminance of their device was 2 300 $cd \cdot m^{-2}$ at 6 V. These data have great academic importance in ONF photonics because they demonstrated the possibility of employing ONFs as active layers in general OLED structures for the first time.

4. OPVs Based on Electrospun ONFs

OPVs have been attracting huge attention in the field of photovoltaics as inexpensive, lightweight, and solution-processable solar cells that can be compatible with flexible substrates.[61–69] Unlike OLEDs, ONFs are largely incorporated in OPVs by diverse preparation methods (e.g., self-assembled polymer nanowires grown from thin films and fabricated via nanolithography, and ONFs fabricated directly via electrospinning) to increase the power conversion efficiency (PCE) of OPVs.[21,23,33,34,70,71] ONFs have many strong points in OPVs, such as huge surface-to-volume ratio, large exciton diffusion length, easy morphology control, and high charge carrier mobilities.[7,61,62] Nevertheless, particularly electrospun ONFs have rarely been employed in OPVs because typically used donor–acceptor blend solutions (e.g., P3HT and fullerene derivatives) cannot provide sufficient chain entanglement for continuous fiber formation in electrospinning process due to their low MW and rigid chemical structure.[33,34] However, electrospinning can still open up new research possibilities in OPVs with its ability to easily fabricate multicomponent ultrathin ONFs from a variety of materials.

Sundarrajan et al. used coaxial electrospinning to fabricate solar cloth made of P3HT and phenyl-C_{61}-butyric acid methyl ester (PCBM) blend nanofibers.[33] To overcome the inability to electrospin P3HT/PCBM blend solutions, the authors introduced PVP as the shell to form core–shell ONFs which contain P3HT/PCBM blend inside as the core. To make photovoltaic cloth, the PVP shell was washed away by soaking in ethanol. The remaining P3HT/PCBM nanofibers had diameters of 0.94 ± 0.18 μm and the cloth showed short circuit current (J_{sc}) of 3.2×10^{-6} $mA \cdot cm^{-2}$, open circuit voltage (V_{oc}) of 0.12 V, fill factor (FF) of 22.1 and PCE of 8.7×10^{-6}%; these are all much lower than those of current state-of-art level.[68,69] This low PCE seems to be mainly attributed to the porous nature of deposited ONF mats, which leads to significant decreases in the volume and total interfacial area of P3HT/PCBM heterojunction when compared with those of thin film. The decreased active volume and total interfacial area cause a significant drop in exciton generation and separation. Furthermore, the nonwoven fiber mat morphology interrupts a charge transport process by limited fiber-to-fiber contacts and scattered transport directions along unaligned fibers. Moreover, poor contact between ONFs and electrodes can be a problem for charge extraction to electrodes.

Significantly increased PCE in a similar system was recently reported by Bedford et al.[34] P3HT/PCBM nanofibers were co-electrospun with PCL shell and later dissolved in cyclopentanone to make pure P3HT/PCBM nanofibers with diameters of 120 ± 30 nm (Figure 5). The nanofiber-incorporated OPVs had improved PCE (4.0%) when compared to the previous result (8.7×10^{-6}%).[33] This PCE value even surpassed that of thin film OPVs with same structure (3.2%). This great improvement is largely attributed to the presence of P3HT/PCBM backfill layer.

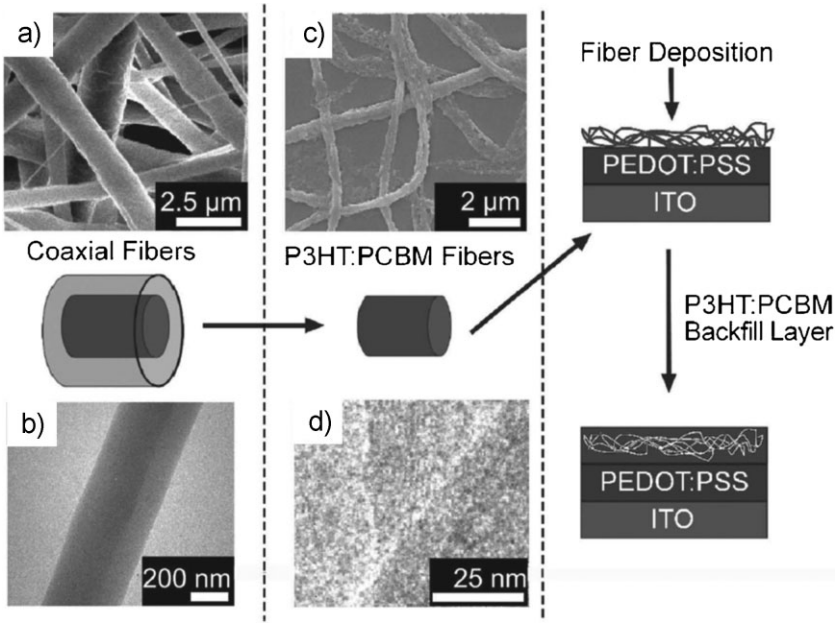

Figure 5. Schematic diagrams showing P3HT/PCBM fiber generation and final device structure. (a) SEM and (b) transmission electron microscope (TEM) image of P3HT/PCBM (core) and PCL (shell) fibers. (c) SEM image and (d) high-resolution TEM image of P3HT/PCBM nanofibers after removal of the PCL shell. Reproduced with permission.[34]

By spin-coating a P3HT/PCBM solution on top of a P3HT/PCBM nonwoven mat, the active volume and donor–acceptor interfacial area could be considerably increased. The charge extraction was also improved by adding a hole transport layer of poly(3,4-ethylenedioxythiophene):poly(styrene sulfonate) (PEDOT:PSS). Furthermore, the increase of PCE over that of thin film devices was explained by the increased optical absorption, caused by the increased in-plane alignment of P3HT chains during electrospinning process.

Some other polymeric nanofibers were demonstrated by electrospinning for future photovoltaic applications. Liu et al. fabricated pure poly[2,5-(2′-ethylhexyloxy)]-1,4-phenylenevinylene (BEH-PPV) nanofibers and BEH-PPV/PCBM composite nanofibers in which alignment was partly induced using a grounded rotating drum.[72] They also prepared uniform and beadless polypyrrolone nanofibers at different concentrations and applied voltages.[73] These studies clearly showed the feasibility of employing high-performance materials other than typical P3HT/PCBM blends when preparing donor–acceptor composite ONFs for fabrication of advanced solar cells.

On the other hand, incorporating inorganic electrospun nanofibers into devices is one of the promising research subjects in the field of organic/inorganic hybrid photovoltaics.[46–48,74] Employing metal oxide materials, such as titanium dioxide (TiO_2),[46] zinc oxide (ZnO),[47,48] and cadmium sulfide (CdS)[74] as electron acceptors can provide many advantages including high charge carrier mobility, low cost, good mechanical and chemical stability, and easy control of size and shape.[46–48] Also, electrospinning offers an easy way to control the porosity and thickness of nanofiber network, which can prevent incomplete infiltration of polymers into the network. The metal oxide materials are usually electrospun with a matrix polymer (usually, PVP) as organic/inorganic composite nanofibers,[46–48] because metal oxide precursor solutions cannot provide enough intermolecular force for fiber formation. Shim et al. fabricated the organic/inorganic hybrid photovoltaic devices where the active layer is composed of multilayer electrospun TiO_2 nanofiber array and MEH-PPV.[46] Hybrid photovoltaic devices based on electrospun ZnO nanofiber network and P3HT were also reported.[47] Tanveer et al. demonstrated the improvement of PCE (2.23%) in P3HT:PCBM/ZnO nanofiber-based photovoltaic cells by optimizing nanofiber mat thickness.[48] The hybrid solar cells with the active layer composed of CdS-coated cellulose acetate fibers and P3HT were recently reported by Cortina et al.[74]

5. OFETs Based on Electrospun ONFs

The OFET is one of the most crucial components for future displays and nanoelectronics because it allows low-cost solution processes for mass production of flexible, large-area devices.[75–82] In OFETs, the electrical characteristics are mainly determined by two important parameters: charge carrier mobilities and on/off ratio. Therefore, because OSC nanofibers have superior field-effect mobilities due to increased π-conjugated molecular stacking along the fiber axis, they may be the best solution for active channels in OFETs to improve their electrical characteristics.[7,9,15,82] Furthermore, FETs based on ONFs are academically very important because they can provide a perfect model for fundamental studies of electrical conduction in 1D structures, and may ultimately contribute to the realization of 1D thread-form devices and woven electronic textiles.

Pinto et al. (2003) first introduced electrospun ONFs in FETs.[50] The authors used camphorsulfonic-acid-doped polyaniline/PEO nanofibers as channels of the OFETs. The individual ONFs had a conductivity of $\approx 10^{-2}$ S · cm^{-1}, but a

measured hole mobility of just 1.4×10^{-4} $cm^2 \cdot V^{-1} \cdot s^{-1}$ in the depletion mode. González and Pinto (2005) further reported FETs based on electrospun P3HT nanofiber (Figure 6a,b).[35] The ONF channel had a length of 54 μm and diameter of ≈670 nm. The devices had hole mobility of 4×10^{-4} $cm^2 \cdot V^{-1} \cdot s^{-1}$ and on/off ratio of ≈7 in the accumulation mode. The low value of on/off ratio caused by the large off-current was explained as a detrimental effect of oxygen doping to the P3HT nanofibers in air. Also, the curved region in the nanofiber channel and non-uniform fiber morphology, shown in Figure 6a, must have greatly affected the low electrical characteristics of the devices. Liu et al. achieved hole mobility of 0.03 $cm^2 \cdot V^{-1} \cdot s^{-1}$ and on/off ratio of 10^3 in the saturation regime in electrospun P3HT nanofiber FETs (Figure 6c–e).[36] The device had a straight and uniform ONF channel with a length of 10 μm and a width of 180 nm, and these characteristics possibly contributed to the far better mobility and on/off ratio than that of the device fabricated by González and Pinto.[35]

Another group tried coaxial electrospinning to fabricate P3HT nanofibers.[37] By supplying extra solvent through the outer nozzle, clogging at the nozzle tip was successfully prevented and uniform P3HT nanofibers with an average diameter of ≈500 nm were obtained. In addition, to achieve continuous production, this group added a binding polymer (PCL) to P3HT solution in various ratios. However, as expected, the pure P3HT nanofiber FET showed the best electrical characteristics: hole mobility of 0.017 $cm^2 \cdot V^{-1} \cdot s^{-1}$ and on/off ratio of 100, and they decreased as increasing the PCL ratio. Based on these results, this group adopted a polyelectrolyte ion-gel gate dielectric layer to improve the electrical characteristics of the ONF devices (Figure 7).[38] An ionic liquid, 1-ethyl-3-methyl-imidazolium bis(trifluoromethylsulfonyl)imide, was mixed with poly(ethyleneglycol) diacrylate and a UV cross-linking initiator to make a UV crosslinkable poly-electrolyte. The polyelectrolyte exhibited a capacitance of 30 $\mu F \cdot cm^{-2}$ at 10 Hz and 1 $\mu F \cdot cm^{-2}$ at 1 MHz; this high capacitance led to an extremely high carrier mobility of ≈2 $cm^2 \cdot V^{-1} \cdot s^{-1}$ and an on/off ratio of ≈10^5, and to low-voltage operation in P3HT/PCL nanofiber FETs. The use of electrospun ONF channels and methacrylated polymer flexible substrate enabled fabrication of mechanically stable ion-gel patterns by facilitating covalent bonding between the ion-gel and the substrate when exposed to UV irradiation.

The field-effect mobility of P3HT nanofibers was further improved by Chen et al.[40] They fabricated FETs based on P3HT nanofibers using a coaxial electrospinning technique with a P3HT core and a PMMA shell. The mobility could be enhanced (hole mobility of 0.192 $cm^2 \cdot V^{-1} \cdot s^{-1}$ and on/off ratio of 4.45×10^4) by tuning the chain packing and orientation of P3HT in nanofibers with a proper control of the shell flow rate and annealing temperature, when compared with previous results[35–37,39] obtained using a similar device structure. P3HT solution-dominant Taylor cone and slower solidification process at a lower shell flow rate (1 $mL \cdot h^{-1}$) resulted higher crystallinity and enhanced π–π stacking with a proper annealing temperature (100 °C), which was verified by wide-angle X-ray scattering, UV–Vis absorption spectra, and polarized photoluminescence (PL)

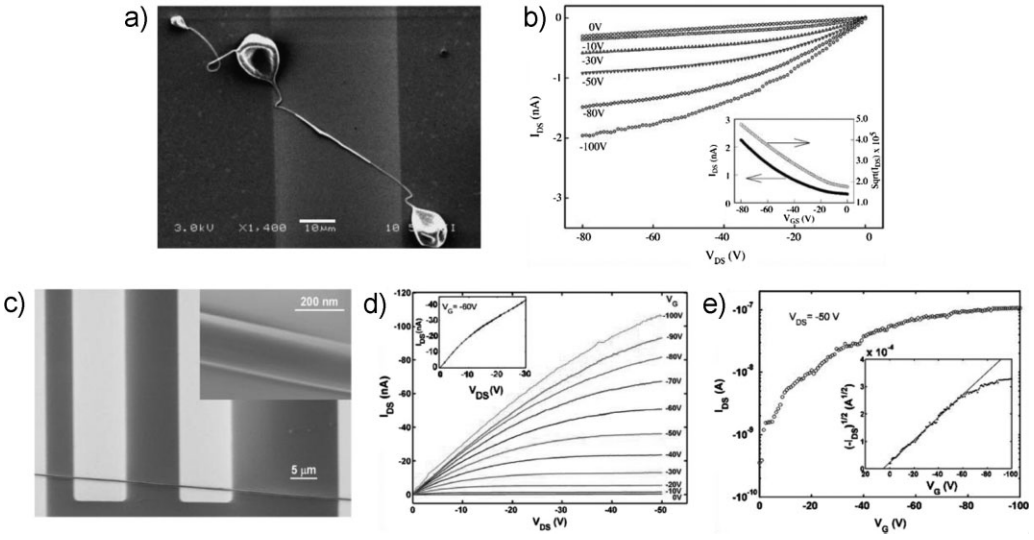

Figure 6. (a) SEM image of electrospun P3HT nanofiber deposited on silver electrode patterned Si/SiO_2 wafer. (b) Output characteristics of the fabricated ONF FET shown in (a); inset: the transfer characteristics of the same device.[35] (c) SEM image of typical electrospun P3HT nanofiber with a diameter of ≈180 nm deposited on gold-electrode-patterned Si/SiO_2 wafer. (d,e) Output characteristics of the fabricated nanofiber FET shown in (c).[36] Reproduced with permission.[35,36] Copyright 2005, Elsevier B. V.[35] and American Institute of Physics.[36]

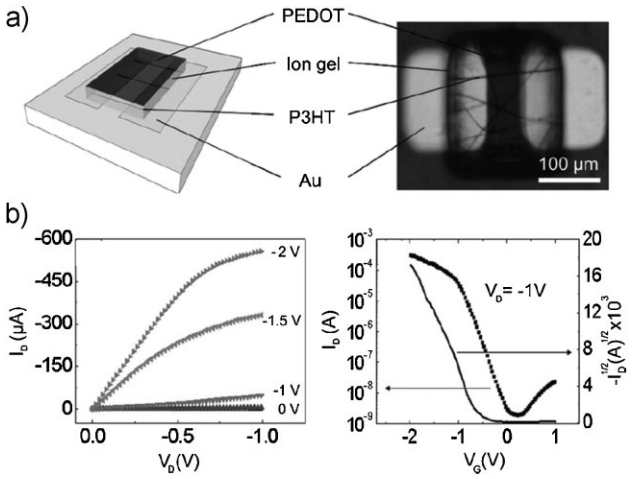

Figure 7. (a) Schematic diagram and OM image showing the device structure with P3HT nanofibers. (b) Output (left) and transfer (right) characteristics of the transistors. Reproduced with permission.[38] Copyright 2010, American Chemical Society.

spectra. This group extended their research by introducing a new 2D thiophene-acceptor conjugated copolymer[83] and crystalline-induced procedure.[9] Lin et al. reported the morphology and charge transport characteristics of electrospun ONFs of poly{[2′,5″-5,5‴-di(2-ethylhexyl)-3′;5′,2″;4″,2‴]quaterthiophene-*alt*-3,6-dithien-2-yl-2,5-di(2-ethylhexyl)-pyrrolo[3,4-c]pyrrole-1,4-dione-5′,5″-diyl]} (P4TDPP).[9] The crystalline-induced procedure included heating to 60 °C for 10 min. and subsequent cooling at 10 °C for 10 min in ultrasonic bath. This procedure was demonstrated to assist the formation of well-packed of P4TDPP chain and small fiber-like crystalline phase, which were confirmed by atomic force microscope and TEM images. They also demonstrated that electrospinning process could result in enhanced π–π molecular stacking and highly ordered orientation of crystallites in ONFs (Figure 8a) with a systematic study of polarized UV–Vis spectroscopy, grazing-incidence X-ray diffraction patterns and in-plane X-ray diffraction profiles. The P4TDPP nanofibers showed a high mobility of 0.305 $cm^2 \cdot V^{-1} \cdot s^{-1}$ and on/off ratio of 1.30×10^5, and this mobility was significantly higher than that of spin-coated film (2.10×10^{-2} $cm^2 \cdot V^{-1} \cdot s^{-1}$).

MEH-PPV is a well-known *p*-type red-light-emitting conjugated polymer. It can be suitable for optoelectronics based on electrospun ONFs because high-MW MEH-PPV can provide sufficient chain entanglement for fiber formation.[39,84] Babel et al. prepared MEH-PPV/P3HT and MEH-PPV/poly(9,9-dioctylfluorene) (PFO) blend nanofibers and studied their morphology and photophysical characteristics.[39] They found that the large interfacial area between MEH-PPV and P3HT in MEH-PPV/P3HT blend nanofibers makes the energy transfer more efficient compared with MEH-PPV/P3HT blend films. This larger interfacial area was resulted from the morphology of the fibers; P3HT nanoparticles of 30–50 nm were dispersed on MEH-PPV fiber matrix (Figure 9a), leading to smaller phase-separated domain size than that in MEH-PPV/P3HT blend films (100–150 nm). On the contrary, core–shell structure of MEH-PPV/PFO blend nanofibers (Figure 9b), which have the insufficient interfacial surface area between MEH-PPV and PFO, caused inefficient energy transfer and broad white light emission. Based on these results, they fabricated OFETs based on MEH-PPV/P3HT nanofiber nonwoven mats, which exhibited the hole mobility in the range of $(0.05–1) \times 10^{-3}$ $cm^2 \cdot V^{-1} \cdot s^{-1}$ after considering effective channel area. Tu et al. (2010) demonstrated the electrospun single MEH-PPV nanofiber FETs (a maximum hole mobility of 5×10^{-3} $cm^2 \cdot V^{-1} \cdot s^{-1}$, and an on/off ratio of up to 780) and showed that PL intensity can be modulated by adjusting the gate voltage.[84] Moreover, they used Fourier transform infrared spectroscopy and polarized PL measurement to analyze the molecular alignment effect in the fibers.

Other than *p*-type conjugated polymers, *n*-type semiconducting polymer fibers were recently reported by Canesi et al.[85] They fabricated smooth poly{[*N*,*N*′-bis(2-octyl-dodecyl)-naphthalene-1,4,5,8-bis(dicarboximide)-2,6-diyl]-*alt*-5,5′-(2,2′-bithiophene)} (P(NDI2OD-T2))/PEO blend nanofibers by means of electrospinning and tested their electrical characteristics for the first time. The P(NDI2OD-T2) nanofiber-based FETs (Figure 10a) exhibited a electron mobility of 0.05–0.09 $cm^2 \cdot V^{-1} \cdot s^{-1}$, which nearly corresponded to that of thin film FETs (0.07–0.08 $cm^2 \cdot V^{-1} \cdot s^{-1}$).

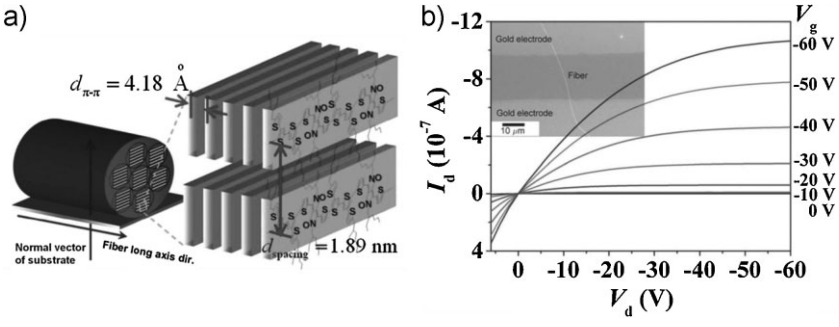

Figure 8. (a) Schematic diagram of molecular packing structure in electrospun P4TDPP nanofibers. (b) Output characteristics of an FET based on electrospun single P4TDPP nanofibers with the crystalline-induced procedure. The inset shows the SEM image of the single P4TDPP nanofiber channel between two gold electrodes. Reproduced with permission.[9]

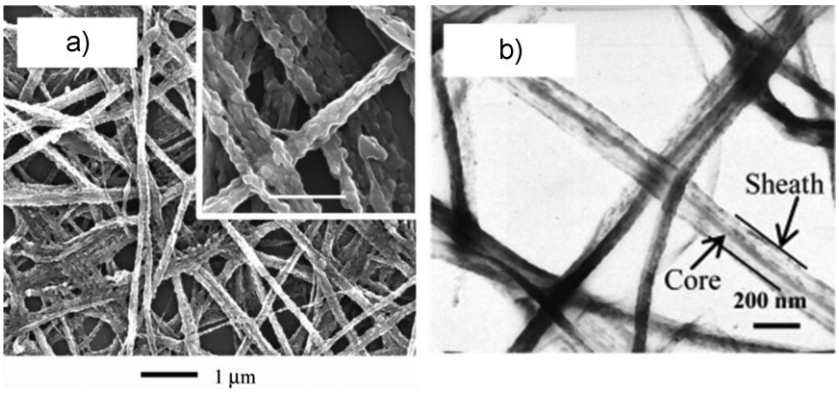

Figure 9. (a) SEM image of electrospun MEH-PPV/P3HT blend nanofibers with 30 wt.-% MEH-PPV. (b) TEM image of electrospun MEH-PPV/PFO blend nanofibers with 44 wt.-% MEH-PPV. Reproduced with permission.[39] Copyright 2005, American Chemical Society.

Uniaxial fiber alignment is a very important issue especially for electrospun ONF-based FETs because randomly oriented structures can be a problem for the microscale device fabrication and channel area definement.[19,86] To efficiently collect the uniaxially aligned ONFs, various alignment techniques have been developed and employed.[19] Among them, the set-up using two parallel separate collectors is most frequently used for the fabrication of electrospun ONF-based FETs[9,37,38,40,84–86] because it is very simple, and the suspended ONFs can be easily transferred to the device substrates.[19] However, until now, perfectly aligned semiconducting ONFs with a constant separation and controlled orientation, which may be crucial for fabricating large-area electronic device arrays, have not realized yet.

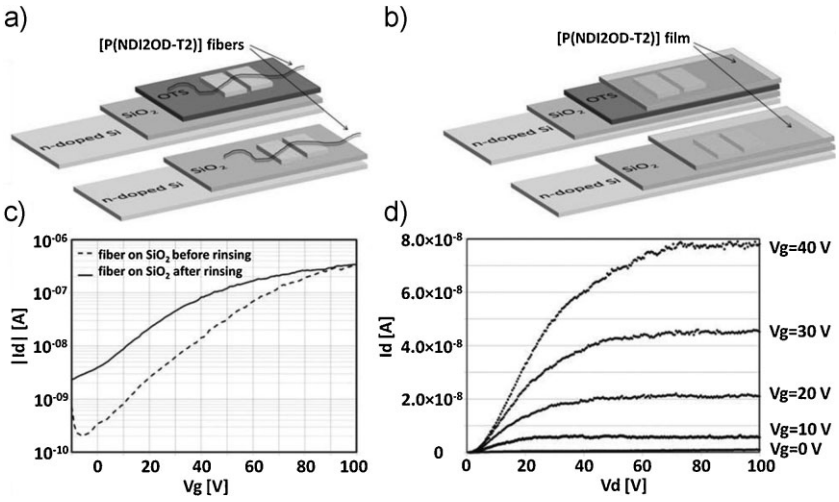

Figure 10. Schematic diagrams of P(NDI2OD-T2) (a) single nanofiber and (b) thin film FETs. (c) The transfer (a drain voltage of 100 V) and (d) output characteristics of the single nanofiber FETs before and after rinsing with acetonitrile. Reproduced with permission.[85] Copyright 2012, American Chemical Society.

6. Lasing Action and Waveguides in Electrospun ONFs

A laser is an acronym for "light amplification by stimulated emission of radiation"; it means a device that emits highly directional and strongly amplified coherent light with very narrow band width. The main mechanism for optically pumped lasing is light oscillation in a gain medium. Specifically, as incident light travels back and forth in an optical cavity, it is coherently amplified by stimulated emission and when the round-trip gain is equal to the round-trip loss, lasing occurs.[87–89]

Over the last few decades, OSCs have been intensively studied in photonics as suitable media for lasers and optical waveguides because OSCs have large cross-sections for strong absorption and stimulated emission, low degree of self-absorption, good optical tunability, and fine processability.[4,5,16,88–97] Especially, many distinguishing features of ONFs make them promising building blocks for lab-on-a-chip experiments including analytical spectroscopy and biomedical diagnostics, and optoelectronic integrated logic circuits in the subwavelength regime.[16,89–91] First, reduced size of ONFs enables submicron-scale light propagation and amplification, which is crucial for photonic communication systems of reduced scale. Also, ONF itself can be a good optical cavity for waveguiding and lasing actions. Optically smooth surfaces and flat end facets of ONFs can make them act as axial Fabry-Pérot cavities. These characteristics can minimize optical loss by effectively suppressing scattering and increasing reflection, particularly for crystalline fibers that are almost free of defects.[89] Because optical cavities with a nanofiber geometry can be directly fabricated by simple fabrication techniques of ONFs, complex and expensive processes, such as e-beam lithography, are not necessary.[4,16] Moreover, 1D high-order stacking of π-conjugated molecules improves the photon-crystal lattice interactions, which facilitates light propagation inside the cavity. In disordered structures, many defects and grain boundaries disturb light propagation by scattering the photons (photon-disordered phase interaction). However, in ONFs, the molecular stacking along the fiber axis might be enhanced due to the

strong stretching force during electrospinning process.[9,84] This consequently results in lower light propagation loss due to more effective confinement inside the crystal and propagation along the π–π stacking direction.[89] Furthermore, 1D nanoscale architectures can facilitate the fundamental studies of 1D optical properties of OSCs. For example, Martini et al. demonstrated that the 1D chain alignment of semiconducting polymers leaded to highly polarized and low-threshold amplified spontaneous emission by confining the chains into the aligned nanopores of a silica host.[98]

However, for lasing action, an ONF cannot be too small because the threshold gain is a strong function of fiber length and diameter.[87,90] Normally, to reach the lasing threshold, the diameter should be larger than ≈200 nm. Furthermore, ONF morphology significantly influences waveguiding and lasing properties.[89,99] In this sense, electrospinning can be a powerful method to directly fabricate ONFs and manipulate their optical properties due to the simple process and facile control over their sizes and morphologies.

These advantages of electrospinning have motivated studies of photonic applications of electrospun ONFs; these applications include optical waveguiding,[99–102] lasing,[28,103,104] and optical anisotropy analysis.[105,106] The light waveguiding effect in electrospun ONFs was efficiently investigated by imaging and by analyzing the PL intensity along the fiber, with a variety of materials such as polymers,[99,101] small molecule/polymer blend,[100] and organic/inorganic composites.[102] The electrospun ONFs have usually shown highly polarized PL emission spectra, thus revealing their anisotropic molecular packing along the fiber axis.[105] Moreover, the optical anisotropy could be further enhanced using room-temperature nanoimprint lithography, a nanoscale patterning technique.[106]

Optically pumped lasing from electrospun gain nanofibers was first demonstrated by Camposeo et al. (2009).[28] Electrospun single PMMA nanofibers doped with an organic fluorescence dye (Rhodamine 6G, R6G) exhibited optical waveguiding in bent structures, and laser emission at 585 nm with extremely narrow full-width-at-half-maximum of 0.3 nm (Figure 11). This group further studied the light emission and propagation properties in electrospun conjugated polymer nanofibers, and observed equal mode spacing of 1.7 nm from a single PMMA/R6G nanofiber; this spacing was evidence of the formation of Fabry-Pérot cavity modes.[103] 3D multimode lasing from dye-doped electrospun PS microfibers at relatively low thresholds was also recently reported.[104]

7. Conclusion

This focused review has illuminated the current state and potential of electrospun ONFs for electronic and photonic applications. Use of ONFs has offered a good chance to investigate the fundamental properties of OSCs and has boosted the development of ONF-based electronics (OLEDs, OPVs, OFETs) and photonics (lasers and waveguides) with their unique advantages. Also, electrospinning opens a very simple and effective way to fabricate ONFs and assess their future potential in many fields such as textile electronics, energy harvesting devices, biosensing devices, lab-on-a-chip devices, and integrated electronic or photonic circuits. However, electrospinning has not been fully explored yet and still many challenges must be solved to achieve practical applications of ONFs.

First, from an academic point of view, electrical and optical properties of 1D organic nanostructures should be more deeply investigated. The mechanism of charge transport in ONFs must be identified using systematic analysis of molecular packing morphology to find ways to further improve their properties. Second, fine control of individual ONFs is absolutely required. Until now, although some techniques to align the nanofibers have been developed, perfect alignment and individual control

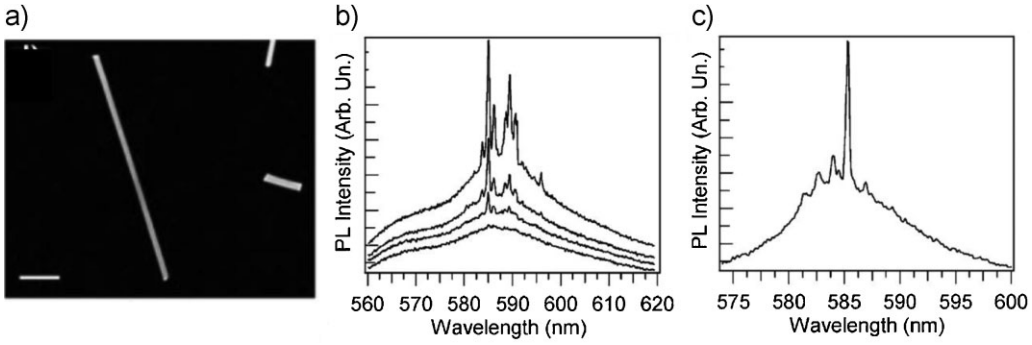

Figure 11. (a) Fluorecence OM image of R6G doped PMMA fibers (b) PL emission spectra of the fibers at different pump fluences. (50, 65, 70, and 100 μJ · cm^{-2}, from bottom to top) (c) PL emission spectrum of a single R6G doped PMMA fiber at a pump fluence of 150 μJ · cm^{-2}. Reproduced with permission.[28] Copyright 2009, WILEY-VCH Verlag GmbH & Co. KGaA, Weinheim.

of semiconducting ONFs have not been realized yet. To realize the practical applications of semiconducting ONF devices, methods must be developed that can fabricate perfectly aligned ONF arrays at desired positions and orientations with high accuracy and reproducibility. Finally, novel organic semiconducting materials must be developed to improve the relatively inferior electrical and optical characteristics of ONF-based devices to those of organic thin film-based devices or inorganic nanowires-based devices and to increase the variety of materials that can be used in electrospinning. In particular, OLEDs based on ONFs have shown lower brightness and efficiency than those of OLEDs based on thin films. Newly designed polymers and small molecules to be developed will effectively enhance the charge transport and luminance properties of the devices. Furthermore, if functional conjugated polymers that induce large chain entanglement can be synthesized, ONFs with useful functionalities could be easily achieved by electrospinning.

At this point, further intensive research is definitely required to overcome these challenges. With deeper investigation into material properties and fabrication processes, electrospun ONFs will be able to satisfy the demands for functional units in nanoelectronics and nanophotonics by achieving maximum potential of OSCs.

Acknowledgements: This work was supported by a grant (Code No. 2012-054547) from the Center for Advanced Soft Electronics under the Global Frontier Research Program of the Ministry of Education, Science and Technology, Korea. This research was also supported by the Converging Research Center Program through the Ministry of Education, Science and Technology (No. 2012K001322). This work was also supported by the POSTECH Basic Science Research Institute Grant.

Received: September 29, 2012; Revised: January 26, 2013; Published online: March 19, 2013; DOI: 10.1002/mame.201200364

Keywords: conjugated polymers; electrospinning; fibers; organic electronics and photonics; organic semiconductor nanowires

[1] Z. Bao, J. A. Rogers, H. E. Katz, *J. Mater. Chem.* **1999**, *9*, 1895.
[2] T. Sekitani, T. Someya, *Adv. Mater.* **2010**, *22*, 2228.
[3] J. A. Rogers, T. Someya, Y. Huang, *Science* **2010**, *327*, 1603.
[4] I. D. W. Samuel, G. A. Turnbull, *Chem. Rev.* **2007**, *107*, 1272.
[5] F. Hide, M. A. Díaz-García, B. J. Schwartz, A. J. Heeger, *Acc. Chem. Res.* **1997**, *30*, 430.
[6] J. Clark, G. Lanzani, *Nat. Photonics* **2010**, *4*, 438.
[7] F. S. Kim, G. Ren, S. A. Jenekhe, *Chem. Mater.* **2011**, *23*, 682.
[8] T.-Q. Nguyen, J. Wu, V. Doan, B. J. Schwartz, *Science* **2000**, *288*, 652.
[9] C. J. Lin, J. C. Hsu, J. H. Tsai, C. C. Kuo, W. Y. Lee, W. C. Chen, *Macromol. Chem. Phys.* **2011**, *212*, 2452.
[10] V. Thavasi, G. Singh, S. Ramakrishna, *Energy Environ. Sci.* **2008**, *1*, 205.
[11] M. Yu, Y.-Z. Long, B. Sun, Z. Fan, *Nanoscale* **2012**, *4*, 2783.
[12] S. Cavaliere, S. Subianto, I. Savych, D. J. Jones, J. Rozière, *Energy Environ. Sci.* **2011**, *4*, 4761.
[13] B. Ding, M. Wang, X. Wang, J. Yu, G. Sun, *Mater. Today* **2010**, *13*, 16.
[14] Y. Wang, A. La, Y. Ding, Y. Liu, Y. Lei, *Adv. Funct. Mater.* **2012**, *22*, 3547.
[15] S. B. Jo, W. H. Lee, L. Qiu, K. Cho, *J. Mater. Chem.* **2012**, *22*, 4244.
[16] A. Camposeo, L. Persano, D. Pisignano, *Macromol. Mater. Eng.* **2012**, DOI: 10.1002/mame.201200277.
[17] D. Li, Y. Xia, *Adv. Mater.* **2004**, *16*, 1151.
[18] A. Greiner, J. H. Wendorff, *Angew. Chem., Int. Ed.* **2007**, *46*, 5670.
[19] W. E. Teo, S. Ramakrishna, *Nanotechnology* **2006**, *17*, R89.
[20] D. O'Carroll, I. Lieberwirth, G. Redmond, *Nat. Nanotechnol.* **2007**, *2*, 180.
[21] B.-G. Kim, M.-S. Kim, J. Kim, *ACS Nano* **2010**, *4*, 2160.
[22] F. Gu, H. Yu, P. Wang, Z. Yang, L. Tong, *ACS Nano* **2010**, *4*, 5332.
[23] M. Aryal, K. Trivedi, W. Hu, *ACS Nano* **2009**, *3*, 3085.
[24] Q. Tang, Y. Tong, W. Hu, Q. Wan, T. Bjørnholm, *Adv. Mater.* **2009**, *21*, 4234.
[25] O. Fenwick, L. Bozec, D. Credgington, A. Hammiche, G. M. Lazzerini, Y. R. Silberberg, F. Cacialli, *Nat. Nanotechnol.* **2009**, *4*, 664.
[26] C. D. Marco, E. Mele, A. Camposeo, R. Stabile, R. Cingolani, D. Pisignano, *Adv. Mater.* **2008**, *20*, 4158.
[27] J. Miao, M. Miyauchi, T. J. Simmons, J. S. Dordick, R. J. Linhardt, *J. Nanosci. Nanotechnol.* **2010**, *10*, 5507.
[28] A. Camposeo, F. Di Benedetto, R. Stabile, A. A. R. Neves, R. Cingolani, D. Pisignano, *Small* **2009**, *5*, 562.
[29] W.-J. Li, C. T. Laurencin, E. J. Caterson, R. S. Tuan, F. K. Ko, *J. Biomed. Mater. Res.* **2002**, *60*, 613.
[30] X.-H. Qin, S.-Y. Wang, *J. Appl. Polym. Sci.* **2006**, *102*, 1285.
[31] S. L. Shenoy, W. D. Bates, H. L. Frisch, G. E. Wnek, *Polymer* **2005**, *46*, 3372.
[32] P. Gupta, C. Elkins, T. E. Long, G. L. Wilkes, *Polymer* **2005**, *46*, 4799.
[33] S. Sundarrajan, R. Murugan, A. S. Nair, S. Ramakrishna, *Mater. Lett.* **2010**, *64*, 2369.
[34] N. M. Bedford, M. B. Dickerson, L. F. Drummy, H. Koerner, K. M. Singh, M. C. Vasudev, M. F. Durstock, R. R. Naik, A. J. Steckl, *Adv. Energy Mater.* **2012**, *2*, 1136.
[35] R. González, N. J. Pinto, *Synth. Met.* **2005**, *151*, 275.
[36] H. Liu, C. H. Reccius, H. G. Craighead, *Appl. Phys. Lett.* **2005**, *87*, 253106.
[37] S. Lee, G. D. Moon, U. Jeong, *J. Mater. Chem.* **2009**, *19*, 743.
[38] S. W. Lee, H. J. Lee, J. H. Choi, W. G. Koh, J. M. Myoung, J. H. Hur, J. J. Park, J. H. Cho, U. Jeong, *Nano Lett.* **2010**, *10*, 347.
[39] A. Babel, D. Li, Y. Xia, S. A. Jenekhe, *Macromolecules* **2005**, *38*, 4705.
[40] J.-Y. Chen, C.-C. Kuo, C.-S. Lai, W.-C. Chen, H.-L. Chen, *Macromolecules* **2011**, *44*, 2883.
[41] D. Li, A. Babel, S. A. Jenekhe, Y. Xia, *Adv. Mater.* **2004**, *16*, 2062.
[42] H. A. Bronstein, C. K. Luscombe, *J. Am. Chem. Soc.* **2009**, *131*, 12894.
[43] R. J. Kline, M. D. McGehee, E. N. Kadnikova, J. Liu, J. M. J. Fréchet, M. F. Toney, *Macromolecules* **2005**, *38*, 3312.

[44] A. M. Ballantyne, L. Chen, J. Dane, T. Hammant, F. M. Braun, M. Heeney, W. Duffy, I. McCulloch, D. D. C. Bradley, J. Nelson, *Adv. Funct. Mater.* **2008**, *18*, 2373.
[45] W. Ma, J. Y. Kim, K. Lee, A. J. Heeger, *Macromol. Rapid Commun.* **2007**, *28*, 1776.
[46] H.-S. Shim, S.-I. Na, S. H. Nam, H.-J. Ahn, H. J. Kim, D.-Y. Kim, W. B. Kim, *Appl. Phys. Lett.* **2008**, *92*, 183107.
[47] S. Wu, Q. Tai, F. Yan, *J. Phys. Chem. C* **2010**, *114*, 6197.
[48] M. Tanveer, A. Habib, M. B. Khan, *Mater. Sci. Eng., B* **2012**, *177*, 1144.
[49] V. Vohra, U. Giovanella, R. Tubino, H. Murata, C. Botta, *ACS Nano* **2011**, *5*, 5572.
[50] N. J. Pinto, A. T. Johnson, Jr., A. G. MacDiarmid, C. H. Mueller, N. Theofylaktos, D. C. Robinson, F. A. Miranda, *Appl. Phys. Lett.* **2003**, *83*, 4244.
[51] H. Yang, C. R. Lightner, L. Dong, *ACS Nano* **2012**, *6*, 622.
[52] A. Dodabalapur, *Solid State Commun.* **1997**, *102*, 259.
[53] C.-T. Chen, *Chem. Mater.* **2004**, *16*, 4389.
[54] S. Chen, L. Deng, J. Xie, L. Peng, L. Xie, Q. Fan, W. Huang, *Adv. Mater.* **2010**, *22*, 5227.
[55] M. C. Gather, A. Köhnen, K. Meerholz, *Adv. Mater.* **2011**, *23*, 233.
[56] T.-H. Han, Y. Lee, M.-R. Choi, S.-H. Woo, S.-H. Bae, B. H. Hong, J.-H. Ahn, T.-W. Lee, *Nat. Photonics* **2012**, *6*, 105.
[57] T.-H. Han, M.-R. Choi, S.-H. Woo, S.-Y. Min, C.-L. Lee, T.-W. Lee, *Adv. Mater.* **2012**, *24*, 1487.
[58] T.-W. Lee, S. Jeon, J. Maria, J. Zaumseil, J. W. P. Hsu, J. A. Rogers, *Adv. Funct. Mater.* **2005**, *15*, 1435.
[59] T.-W. Lee, J. Zaumseil, Z. Bao, J. W. P. Hsu, J. A. Rogers, *Proc. Natl. Acad. Sci. USA* **2004**, *101*, 429.
[60] J. M. Moran-Mirabal, J. D. Slinker, J. A. DeFranco, S. S. Verbridge, R. Ilic, S. Flores-Torres, H. Abruña, G. G. Malliaras, H. G. Craighead, *Nano Lett.* **2007**, *7*, 458.
[61] C. J. Brabec, *Sol. Energy Mater. Sol. Cells* **2004**, *83*, 273.
[62] B. Kippelen, J.-L. Brédas, *Energy Environ. Sci.* **2009**, *2*, 241.
[63] L.-M. Chen, Z. Hong, G. Li, Y. Yang, *Adv. Mater.* **2009**, *21*, 1434.
[64] C. J. Brabec, S. Gowrisanker, J. J. M. Halls, D. Laird, S. Jia, S. P. Williams, *Adv. Mater.* **2010**, *22*, 3839.
[65] J. Weickert, R. B. Dunbar, H. C. Hesse, W. Wiedemann, L. Schmidt-Mende, *Adv. Mater.* **2011**, *23*, 1810.
[66] T.-W. Lee, K.-G. Lim, D.-H. Kim, *Electron. Mater. Lett.* **2010**, *6*, 41.
[67] J. H. Park, T.-W. Lee, B.-D. Chin, D. H. Wang, O. O. Park, *Macromol. Rapid Commun.* **2010**, *31*, 2095.
[68] L. Dou, J. You, J. Yang, C.-C. Chen, Y. He, S. Murase, T. Moriarty, K. Emery, G. Li, Y. Yang, *Nat. Photon.* **2012**, *6*, 180.
[69] Z. He, C. Zhong, S. Su, M. Xu, H. Wu, Y. Cao, *Nat. Photon.* **2012**, *6*, 591.
[70] H.-S. Wang, L.-H. Lin, S.-Y. Chen, Y.-L. Wang, K.-H. Wei, *Nanotechnology* **2009**, *20*, 075201.
[71] Q. H. Cui, L. Jiang, C. Zhang, Y. S. Zhao, W. Hu, J. Yao, *Adv. Mater.* **2012**, *24*, 2332.
[72] H. A. Liu, D. Zepeda, J. P. Ferraris, K.J. Balkus, Jr., *ACS Appl. Mater. Interfaces* **2009**, *1*, 1958.
[73] X. L. Wang, X. D. Bai, X. K. Jiang, C. Wang, C. Chen, *Pig. Resin Technol.* **2010**, *39*, 262.
[74] H. Cortina, C. Martínez-Alonso, M. Castillo-Ortega, H. Hu, *Mater. Sci. Eng., B* **2012**, *177*, 1491.
[75] G. Horowitz, *Adv. Mater.* **1998**, *10*, 365.
[76] A. Dodabalapur, *Mater. Today* **2006**, *9*, 24.
[77] Y. Cao, M. L. Steigerwald, C. Nuckolls, X. Guo, *Adv. Mater.* **2010**, *22*, 20.
[78] Y. Wen, Y. Liu, *Adv. Mater.* **2010**, *22*, 1331.
[79] Y. Guo, G. Yu, Y. Liu, *Adv. Mater.* **2010**, *22*, 4427.
[80] T.-W. Lee, Y. Byun, B.-W. Koo, I.-N. Kang, Y.-Y. Lyu, C. H. Lee, L. Pu, S. Y. Lee, *Adv. Mater.* **2005**, *17*, 2180.
[81] T.-W. Lee, J. H. Shin, I.-N. Kang, S. Y. Lee, *Adv. Mater.* **2007**, *19*, 2702.
[82] A. L. Briseno, S. C. B. Mannsfeld, S. A. Jenekhe, Z. Bao, Y. Xia, *Mater. Today* **2008**, *11*, 38.
[83] J.-H. Tsai, W.-Y. Lee, W.-C. Chen, C.-Y. Yu, G.-W. Hwang, C. Ting, *Chem. Mater.* **2010**, *22*, 3290.
[84] D. Tu, S. Pagliara, A. Camposeo, L. Persano, R. Cingolani, D. Pisignano, *Nanoscale* **2010**, *2*, 2217.
[85] E. V. Canesi, A. Luzio, B. Saglio, A. Bianco, M. Caironi, C. Bertarelli, *ACS Macro Lett.* **2012**, *1*, 366.
[86] D. Li, Y. Wang, Y. Xia, *Nano Lett.* **2003**, *3*, 1167.
[87] M. A. Zimmler, F. Capasso, S. Müller, C. Ronning, *Semicond. Sci. Technol.* **2010**, *25*, 024001.
[88] A. J. Heeger, *Solid State Commun.* **1998**, *107*, 673.
[89] Q. H. Cui, Y. S. Zhao, J. Yao, *J. Mater. Chem.* **2012**, *22*, 4136.
[90] Y. S. Zhao, H. Fu, A. Peng, Y. Ma, Q. Liao, J. Yao, *Acc. Chem. Res.* **2010**, *43*, 409.
[91] F. Quochi, *J. Opt.* **2010**, *12*, 024003.
[92] F. Hide, M. A. Díaz-García, B. J. Schwartz, M. R. Anderson, Q. Pei, A. J. Heeger, *Science* **1996**, *273*, 1833.
[93] M. D. McGehee, A. J. Heeger, *Adv. Mater.* **2000**, *12*, 1655.
[94] C. Zhang, Y. S. Zhao, J. Yao, *Phys. Chem. Chem. Phys.* **2011**, *13*, 9060.
[95] Y. C. Kim, T.-W. Lee, O. O. Park, C. Y. Kim, H. N. Cho, *Adv. Mater.* **2001**, *13*, 646.
[96] T.-W. Lee, O. O. Park, D. H. Choi, H. N. Cho, Y. C. Kim, *Appl. Phys. Lett.* **2002**, *81*, 424.
[97] T.-W. Lee, O. O. Park, H. N. Cho, D. Y. Kim, Y. C. Kim, *J. Appl. Phys.* **2003**, *93*, 1367.
[98] I. B. Martini, I. M. Craig, W. C. Molenkamp, H. Miyata, S. H. Tolbert, B. J. Schwartz, *Nat. Nanotechnol.* **2007**, *2*, 647.
[99] F. D. Benedetto, A. Camposeo, S. Pagliara, E. Mele, L. Persano, R. Stabile, R. Cingolani, D. Pisignano, *Nat. Nanotechnol.* **2008**, *3*, 614.
[100] K. P. Dhakal, H. Lee, J. W. Lee, J. Joo, M. Guthold, J. Kim, *J. Appl. Phys.* **2012**, *111*, 123504.
[101] L. Li, X. Yang, L. Yuan, *Mater. Lett.* **2012**, *66*, 292.
[102] H. Liu, J. B. Edel, L. M. Bellan, H. G. Craighead, *Small* **2006**, *2*, 495.
[103] S. Pagliara, A. Camposeo, F. Di Benedetto, A. Polini, E. Mele, L. Persano, R. Cingolani, D. Pisignano, *Superlattices Microstruct.* **2010**, *47*, 145.
[104] A. J. Das, C. Larfargue, M. Lebental, J. Zyss, K. S. Narayan, *Appl. Phys. Lett.* **2011**, *99*, 263303.
[105] S. Pagliara, M. S. Vitiello, A. Camposeo, A. Polini, R. Cingolani, G. Scamarcio, D. Pisignano, *J. Phys. Chem. C* **2011**, *115*, 20399.
[106] S. Pagliara, A. Camposeo, E. Mele, L. Persano, R. Cingolani, D. Pisignano, *Nanotechnology* **2010**, *21*, 215304.